

Comparative evaluation of different methods for determining the specific surface area of carbon materials used in electrochemical systems

© Pavel V. Oskin^a✉, Roman V. Lepikash^a, Tatyana P. Dyachkova^b, Sergey V. Alferov^a

^a Tula State University, 92, Lenin Av., Tula, 300012, Russian Federation,

^b Tambov State Technical University, Bld. 2, 106/5, Sovetskaya St., Tambov, 392000, Russian Federation

✉ pavelfraj@yandex.ru

Abstract: In this paper, a comparative analysis of methods for determining the surface area in relation to electrode materials was carried out on the example of commercial carbon felts of various structures. For a more complete analysis, scanning electron microscopy and Raman spectroscopy methods were additionally used. It is shown that electrochemical methods for determining the surface area are selective with respect to the edge plane of graphite, which can be both an advantage and a disadvantage, depending on the objectives of the study. It is revealed that the use of the classical method of low-temperature adsorption of gases is not always justified due to the complexity of selecting the correct model describing the system under study. Adsorption of dyes from aqueous solutions seems to be the most suitable method for determining the wetted surface of the material, however, it requires large amounts of sample and is characterized by a significant error.

Keywords: carbon fiber; surface area; electron transfer rate; capacity of the double electric layer; basal plane of graphite; edge plane of graphite; adsorption of methylene blue.

For citation: Oskin PV, Lepikash RV, Dyachkova TP, Alferov SV. Comparative evaluation of different methods for determining the specific surface area of carbon materials used in electrochemical systems. *Journal of Advanced Materials and Technologies*. 2024;9(3):167-176. DOI: 10.17277/jamt.2024.03.pp.167-176

Сравнительная оценка различных методов определения удельной площади поверхности углеродных материалов, использующихся в электрохимических системах

© П. В. Оськин^a✉, Р. В. Лепикаш^a, Т. П. Дьячкова^b, С. В. Алферов^a

^a Тульский государственный университет,
пр. Ленина, 92, Тула, 300012, Российская Федерация,

^b Тамбовский государственный технический университет,
ул. Советская, 106/5, пом. 2, Тамбов, 392000, Российская Федерация

✉ pavelfraj@yandex.ru

Аннотация: В данной работе проведено сравнение методов определения площади поверхности применительно к электродным материалам на примере коммерческих углеродных войлоков различной структуры. Для более полного анализа дополнительно привлечена сканирующая электронная микроскопия, позволившая охарактеризовать морфологию поверхности материала и спектроскопия комбинационного рассеяния, с помощью которой оценивали количество дефектов в кристаллической структуре углерода, а также содержание аморфной фазы. Показана селективность электрохимических методов определения площади поверхности по отношению к краевой плоскости графита, что может являться как преимуществом, так и недостатком, в зависимости от целей исследования. Выявлено, что применение классического метода низкотемпературной адсорбции газов далеко не всегда оправдано, ввиду сложности подбора корректной модели, описывающей исследуемую систему. Кроме того, при исследовании приведенным методом электродных материалов полученные данные будут сильно

завышены из-за лучшей смачиваемости углеродного материала азотом, чем водой. Адсорбция красителей из водных растворов, по-видимому, является наиболее подходящим методом для определения смоченной поверхности материала, однако требует наличия большого числа образцов, характеризуется значительной погрешностью и может давать несколько завышенные результаты, хоть и меньшие, чем низкотемпературная адсорбция азота.

Ключевые слова: углеродное волокно; площадь поверхности; скорость переноса электронов; емкость двойного электрического слоя; базальная плоскость графита; краевая плоскость графита; адсорбция метиленового голубого.

Для цитирования: Oskin PV, Lepikash RV, Dyachkova TP, Alferov SV. Comparative evaluation of different methods for determining the specific surface area of carbon materials used in electrochemical systems. *Journal of Advanced Materials and Technologies*. 2024;9(3):167-176. DOI: 10.17277/jamt.2024.03.pp.167-176

1. Introduction

Specific surface area is one of the key parameters of carbon materials. Various methods are used to determine it. For example, for quasi-one-dimensional materials, it is possible to estimate the specific surface area based on the average fiber radius values [1–3]. However, the geometric estimate cannot be considered accurate, since it does not take into account the heterogeneity of the fiber surface. Low-temperature gas adsorption data [2, 4, 5] and dye adsorption from aqueous solutions [6, 7] are often used. In addition, a number of sources report on electrochemical methods for estimating the specific surface area [8, 9].

The results obtained by the Brunauer–Emmett–Teller (BET) method are often poorly suited for describing the electrochemical behavior of a carbon material due to the difference in the mechanisms of interaction between gas and electrolyte with carbon. Data on dye adsorption from solutions are more suitable in this sense, but difficulties with selecting a physical model of the process remain.

Electrochemical methods are free from this drawback, but require the use of accurate values of a number of constants. Moreover, if the diffusion coefficient used in calculations according to the

Randles-Shevchik equation [8] is known for most standard redox systems, then determining the specific capacity of the electric double layer (EDL) causes difficulties, since this value is made up of the capacities of the marginal and basal planes [10–12], data on which vary significantly in different sources (Table 1). For example, experimentally determined values of the capacity of the marginal plane differ by orders of magnitude due to the contribution of pseudocapacitance [13, 14].

Thus, all currently available methods for assessing the surface area of carbon materials have shortcomings. At the same time, the use of several complementary methods can provide reliable useful information, for example, the ratio of the areas of the basal and edge planes of graphite. This parameter is extremely important for characterizing the electrochemical properties of carbon materials. Thus, in [18], it was shown that materials with a high proportion of the edge plane are able to more effectively reduce oxygen in the cathode space of fuel cells. The rate of electron transfer in redox systems, for example, $[\text{Fe}(\text{CN})_6]^{3-}/[\text{Fe}(\text{CN})_6]^{4-}$ containing ascorbic acid or hydrazine significantly, depend on this ratio [19–21].

Table 1. Specific capacity of the basal and edge plane of graphite

Electrolyte	Basal plane capacity, $\mu\text{F}\cdot\text{cm}^{-2}$	Edge plane capacity, $\mu\text{F}\cdot\text{cm}^{-2}$	Reference
0,9 H NaF	3	50–70	[15]
1 mM HCF in 1M KCl	1–2	70	[11]
1M KCl	0.81	–	[16]
6 M LiCl	4.72 ± 0.37	430.1 ± 9.9	[13]
0,1 M Na_2HPO_4 (pH = 7), 0,1M KCl	4	10^5	[14]
6 M LiCl	4.3–6.0	–	[10]
6 M LiCl	1.7 ± 0.2	25 ± 6	[17]

Usually, the proportion of the edge plane is calculated from the value of the rate constant of heterogeneous electron transfer in the $[\text{Fe}(\text{CN})_6]^{3-}/[\text{Fe}(\text{CN})_6]^{4-}$ system according to equation (1) [11, 12].

$$k = k_e f_e + k_b (1 - f_e), \quad (1)$$

where k is the rate constant of heterogeneous electron transfer, $\text{cm}\cdot\text{s}^{-1}$; k_e is the rate constant of heterogeneous electron transfer to the edge plane of graphite, $\text{cm}\cdot\text{s}^{-1}$; k_b is the rate constant of heterogeneous electron transfer to the basal plane, $\text{cm}\cdot\text{s}^{-1}$; f_e is the fraction of the edge plane of graphite. This method is not very accurate due to the large error in determining the rate constant [22].

According to [1, 16], the fraction of the edge plane is also included in equation (2):

$$C = f_e C_e + (1 - f_e) C_b, \quad (2)$$

where C is the specific capacitance of the EDL for the material, $\mu\text{F}\cdot\text{cm}^{-2}$; C_e is the specific capacitance of the edge plane of graphite, $\mu\text{F}\cdot\text{cm}^{-2}$; C_b is the specific capacitance of the basal plane of graphite, $\mu\text{F}\cdot\text{cm}^{-2}$.

However, it is not possible to use equation (2) in practice due to the complexity of determining the exact value of the specific capacitance of the edge plane EDL.

The aim of this work was to compare different methods for determining the surface area for characterizing carbon materials that can be used in electrochemical systems in the future. Carbon felt was chosen as a model material, since it is widely used in the creation of supercapacitors [23, 24], electrochemical [5, 25] and bioelectrochemical [4, 26] current sources, as well as electrochemical sensors [8].

2. Materials and Methods

2.1. Initial materials and reagents

In this work, two commercial samples of carbon felt obtained by pyrolysis of polyacrylonitrile fiber in an inert atmosphere were investigated. Sample No. 1 was produced by Heibei Huasheng Felt Co Ltd. (China), sample No. 2 was produced by Kompozit-Polymer (Russia).

The reagents (methylene blue, potassium hexacyanoferrate (III), potassium chloride) used in the work were of analytical grade. All solutions were prepared with deionized water and stored in dark glassware at a temperature of 4 °C for no more than a week.

2.2. Analytical methods

Electron images were obtained on a JSM-6510 LV microscope (JEOL, Japan) in low vacuum mode (30 Pa) with secondary electron (SE) registration. Raman spectra were recorded on a DXR Raman Microscope (Thermo Scientific, USA) using a laser with a wavelength of 532 nm.

The surface area was determined by the adsorption of methylene blue (solution concentration $1 \text{ mmol}\cdot\text{dm}^{-3}$) according to the procedure [6] using an SF-2000 spectrophotometer (OKB-Spectr, Russia). The optical density of the dye was measured at a wavelength of 616 nm. The surface area was determined by nitrogen adsorption using a Quantochrome Autosorb IQ Nova 1200e specific surface area and porosity analyzer (Quantochrome Instruments, USA) at a temperature of 77 K and a partial pressure of 0.05 – 0.30. Electrochemical measurements were performed on a CORRTTEST CS1350 potentiostat-galvanostat (Corrtest, China) in a three-electrode cell with a saturated silver chloride electrode as the reference electrode and a $0.5 \times 0.5 \times 0.1$ cm platinum foil as the auxiliary electrode. A 0.1 M KCl solution was used as the background electrolyte. The concentration of potassium hexacyanoferrate (III) in the solution was 0.5 mM. Cyclic voltammograms were recorded at scan rates of $10\text{--}500 \text{ mV}\cdot\text{s}^{-1}$ in the range of $-0.4\text{--}+0.6$ V.

Impedance spectra were recorded in 0.1 M KCl in the frequency range from 1 Hz to 0.1 MHz at the anodic potentials of cyclic voltammograms (CV) of potassium hexacyanoferrate (III) (to determine the rate constant of heterogeneous transfer) and at the open circuit potential (to determine the specific capacitance of the EDL). The voltage amplitude was 10 mV.

From the CV data, the rate constant of heterogeneous electron transfer was calculated using the Nicholson-Lavagnini method [27, 28] based on the slope of the dependence of the limiting current on $1/\psi$ in accordance with equation (3) obtained by combining the Nicholson and Randles-Shevchik equations:

$$I_p = 0.4463 n F S C \sqrt{1 - \alpha} \frac{k_s \sqrt{\pi}}{\psi}, \quad (3)$$

where I_p is limiting anode current; π is a mathematical constant, 3,14; $1 - \alpha$ is an electron transfer coefficient for the anode process; k_s is a rate constant of heterogeneous electron transfer; F is the Faraday number; S is the electrode area; n is the number of electrons participating in the reaction.

The parameter ψ was determined using equation (4) [28]:

$$\psi = -\frac{-0.6288 + 0.002\Delta E}{1 - 0.017\Delta E}, \quad (4)$$

where ψ is the Nicholson coefficient, V; ΔE is the difference between the potentials of the anodic and cathodic peaks, V.

From the electrochemical impedance spectroscopy data, the rate constant of heterogeneous electron transfer was calculated using equation (5) [27]:

$$k_s = \frac{RT}{R_F n^2 F^2 SX}, \quad (5)$$

where R is the universal gas constant, J·mol·K⁻¹; T is the temperature, K; R_F is the Faraday resistance of the reaction, Ohm; X is the concentration of the electro-active substance in the solution, mol·dm⁻³. To find the Faraday resistance, the Voigt ladder diagram was used. To calculate the specific capacity of the EDL, the Randles diagram was used [29].

Based on the results of the CV with a linear potential sweep at a potential sweep rate of 100 mV·s⁻¹ in the range of 0–0.5 V, the specific capacitance of the EDL of carbon felt was determined using equation (6) [30]:

$$C = \frac{\int_{E_1}^{E_2} I dE}{m(E_2 - E_1)}, \quad (6)$$

where I is the equation for the dependence of current on potential, A; E_1 is the initial potential of the cyclic voltammogram, V; E_2 is the final potential of the voltammogram, V; m is the mass of felt, g.

Charge-discharge curves were recorded at a charge-discharge current of 10 μ A in the potential range of 0–0.5 V. The specific capacity of the EDL was calculated using formula (7) [30]:

$$C = \frac{I'\Delta t}{m\Delta E'}, \quad (7)$$

where I' is the charging (discharging) current, A; Δt is the charging (discharging) time, s; $\Delta E'$ is the absolute value of the difference between the potential at the beginning and end of charging (discharging), V.

3. Results and Discussion

Scanning electron images (SEM) were obtained to characterize the morphology of the felt samples (Fig. 1). Both samples consist of interwoven carbon

fibers with a diameter of about 20 μ m. On the surface of these fibers, longitudinal grooves with a width of 0.1–0.3 μ m are observed, which apparently formed during the production of polyacrylonitrile fiber. On the surface of sample No. 2, growths with a size of 0.5–5.0 μ m are observed. The obtained results are consistent with the literature data [1].

The Raman spectra (Fig. 2) of both samples contain the G (1550 cm⁻¹) and D (1350 cm⁻¹) bands, which are characteristic of all carbon materials. The G band is due to vibrations of sp²-hybridized carbon atoms in the crystal structure of graphite, and the D band is due to the presence of defects in this structure. The degree of defectiveness of a carbon material is usually estimated by the intensity ratio of these bands (I_D/I_G) [31]. The Raman spectrum of sample No. 1 (Fig. 2a) is characterized by a high noise level, which may be a consequence of the amorphization of the structure [31]. This is confirmed by the presence of the D'' peak (1400 cm⁻¹) between the D and G bands, the intensity of which depends on the amount of the bulk amorphous phase in the structure [32]. The Raman spectrum of sample No. 2 (Fig. 2b) additionally contains the $2D$ (2700 cm⁻¹) and $D + G$ (2950 cm⁻¹) bands, characteristic of the ordered structure of graphite [33]. Thus, sample No. 1 is amorphized to a greater extent than sample No. 2. To confirm this conclusion, peaks D' (1600 cm⁻¹) and D'' , were additionally identified using mathematical processing of the Raman spectra in accordance with [34]. The defect density (n_D) [35], the distance between defects (L_d) [35] and the crystallite size (L_D) [36] were also calculated (Table 2).

The I_D/I_G ratio for both materials, the distance between defects, the density of defects and the sizes of crystallites differ slightly, which indicates the similarity of the general parameters of the structure disorder [31]. At the same time, judging by the value of $I_D/I_{D'}$ and the intensity of the D' band, surface [37, 38] rather than intracrystalline [31] defects of the graphite structure are more characteristic of sample No. 2. It is not entirely correct to compare the obtained absolute numerical values of the parameters given in Table 2 with the literature data due to the individual settings of each specific Raman spectrometer [39].

The specific surface area values were measured in various ways for the carbon felt samples, which were then compared with the literature data for analogs (Table 3).

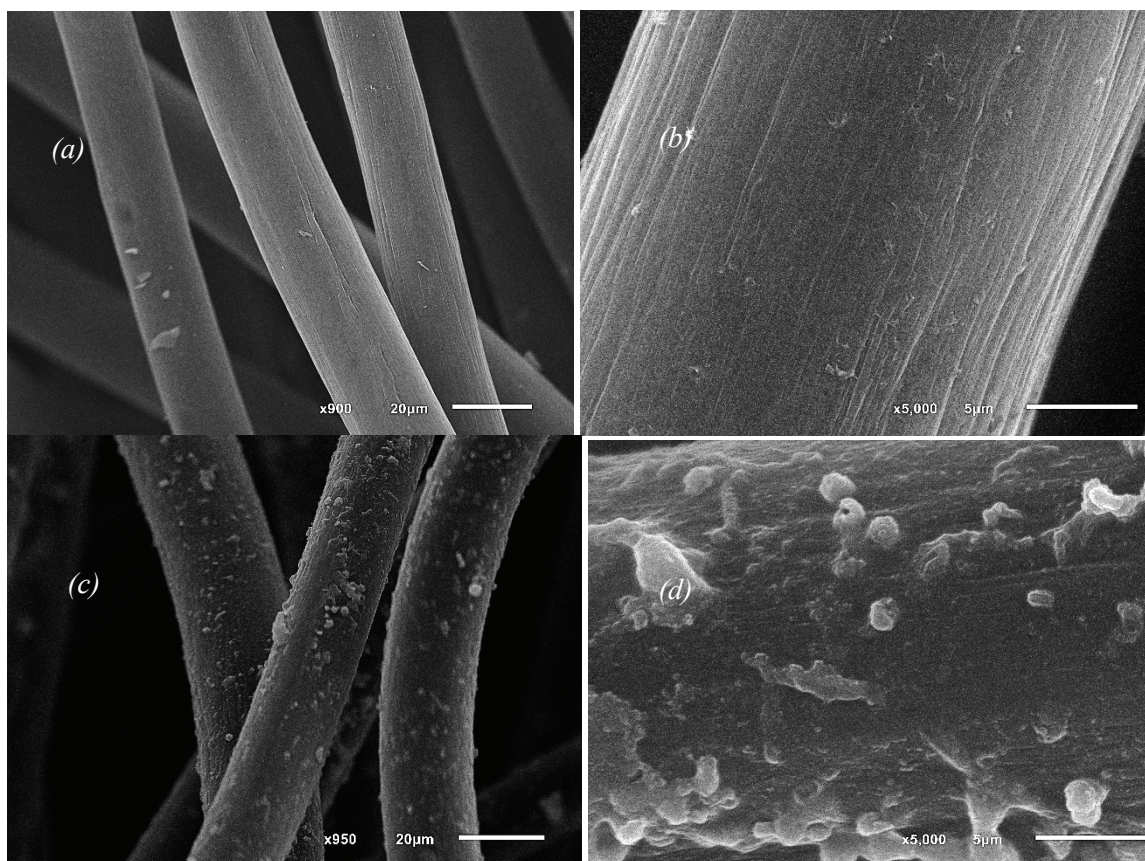


Fig. 1. SEM images of carbon felt samples No. 1 (*a, b*) and No. 2 (*c, d*)

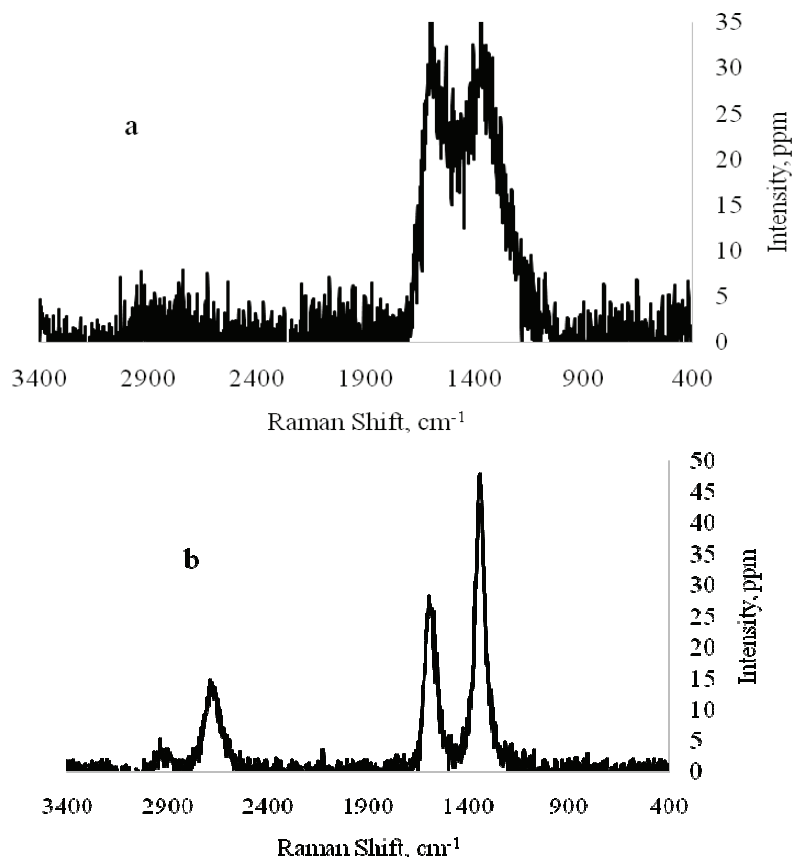


Fig. 2. Raman spectra of sample No. 1 (*a*) and sample No. 2 (*b*)

Table 2. Results of processing the Raman spectra of carbon and graphite felts

Sample	I_D/I_G	L_D , nm	$n_D \cdot 10^{-10}$, cm^{-2}	L_a , nm	$I_{D'}/I_G$	$I_{D''}/I_G$	$I_D/I_{D'}$	Type of defects
1	1.6 ± 0.1	33 ± 2	2.7 ± 0.2	10 ± 2	1.8 ± 0.4	0.7 ± 0.1	1.0 ± 0.2	Local
2	1.8 ± 0.2	32 ± 4	3.1 ± 0.3	9 ± 2	0.3 ± 0.1	–	6.1 ± 0.2	Regional, vacancies

Table 3. Specific surface area of carbon felt determined by various methods

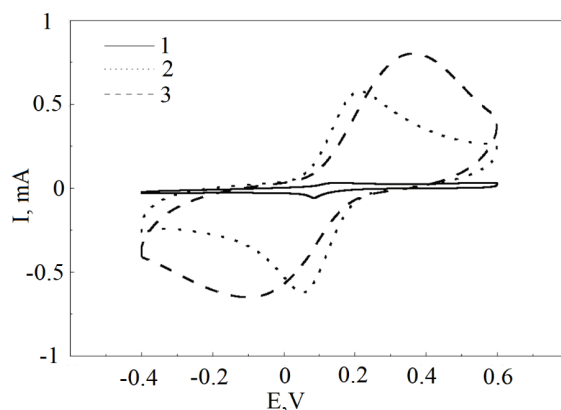
Method	Specific surface area, $\text{m}^2 \cdot \text{g}^{-1}$		References
	Sample No. 1	Sample No. 2	
Nitrogen adsorption (BET)	–	–	0.4 [2]; 1.69 [4]; 0.5 [5]; 0.8 [25]; 1 [24]
Geometrical evaluation	0.011	0.011	0.028 [1]; 0.022 [3]
Methylene blue adsorption	4.5 ± 0.7	4.3 ± 0.4	–
Rendles-Szewczyk equation	0.072 ± 0.006	0.19 ± 0.02	–

It was not possible to determine the surface area by low-temperature gas adsorption due to the extremely long establishment of equilibrium (more than 3 days), which makes it impossible to use the BET model and other common models. Similar cases have already been encountered previously [1], so for comparison with the electrochemical determination it was decided to use a geometric estimate and the adsorption of methylene blue. The surface area was estimated geometrically by calculating the lateral area of an ideally smooth cylinder, which was taken to be carbon fiber. For this calculation, it is necessary to know the density of the felt, which was taken to be $1.9 \text{ g} \cdot \text{cm}^{-3}$ based on literary data [1, 2]. The fiber diameter (Fig. 1) of both graphite and carbon felt is the same and is about $20 \mu\text{m}$, which is why the geometric estimate gives a similar result. However, it should be noted that the use of this approximation for sample No. 2 is incorrect due to the presence of a large number of growths on the surface of its fibers (Fig. 2).

Methylene blue adsorption also yields similar surface area values ((4.5 ± 0.7) and $(4.3 \pm 0.4) \text{ m}^2 \cdot \text{g}^{-1}$), which are an order of magnitude higher than the literature data on low-temperature nitrogen adsorption processed using the BET model (Table 3). The fact that surface area values obtained by different methods differ for carbon materials is widely known [2, 40]. In addition, as mentioned above, low-temperature nitrogen adsorption may yield incorrect results. From the electron microscopy data (Fig. 1), it is evident that the felts should have different surface areas, which does not correlate with the results of determination by methylene blue adsorption. This is

explained by the higher content of defects in the structure of sample No. 1 (from the Raman spectra). In [16], it was shown that defects in the structure of the carbon material are methylene blue adsorption centers. In addition, the use of the methylene blue method for determining the specific surface area can give strong errors towards overestimation in the case of the presence of relatively narrow mesopores in the material due to the interaction between molecules and their conformations in the pores.

The electrochemically active surface area determined using the Randles-Shevchik equation is two orders of magnitude lower than the result obtained by adsorption of methylene blue. Apparently, this is connected with the high rate constant of heterogeneous electron transfer to the edge surface of graphite, due to which only the area of the edge plane is determined, whereas dye adsorption yields the total area.

**Fig. 3.** Voltammograms of an empty wire hook (1), sample 1 (2) and sample 2 (3), scanning speed $100 \text{ mV} \cdot \text{s}^{-1}$

This is consistent with the data of [2], in which the surface area according to BET (total area) and the EDL capacitance (edge plane area) are similarly different. The ratio of the EDL capacitances of different felts can be estimated from the appearance of cyclic voltammograms (Fig. 3). In sample No. 2, the peaks are broadened, which indicates high EDL charging currents, from which one can conclude that the EDL capacitance is higher.

To confirm this conclusion, the specific capacity of the EDL of carbon felt was determined using cyclic voltammetry, electrochemical impedance spectroscopy and charge-discharge curves (Table 4).

The values of the EDL specific capacity determined by different methods are in satisfactory agreement with each other. A slight underestimation of the value obtained by the cyclic voltammetry method may be due to the fact that the potential increases faster than the diffusion of ions from the solution, so the EDL is not charged to the maximum possible value [41]. The specific capacity of the EDL for the “Composite-Polymer” felt is higher, which agrees with the qualitative assessment of the ratio of the EDL capacitances based on the shape of the cyclic voltammograms.

To calculate the rate constants using formulas (3) and (5), the surface area determined using the Randles-Shevchik equation was used. It is directly related to the limiting current, from the dependence

of which on the parameter ψ the constant is calculated.

The results obtained by the two methods (Table 5) are quite close to each other and correspond to the literature data, including those obtained using mathematical models [5, 42] and on electrodes consisting of individual fibers [3].

Thus, the data presented in Table 5 shows that there is no need to use complex mathematical models and single-fiber electrodes [3]. According to the literature data, a high error in determination is characteristic of the rate constant of heterogeneous electron transfer [3, 43]. It can be associated with the heterogeneity of the distribution of the marginal and basal plane in different parts of the felt [2].

An important characteristic of electrochemical properties of carbon materials is the ratio of the edge and basal planes of graphite. As was said above, in a number of redox-active systems, electron transfer occurs only on the edge surface. The percentage of the edge plane area was calculated from the values of the heterogeneous transfer rate constant according to equation (2), the capacity of the EDL – according to equation (1), and also from the ratio of the specific surface areas determined by the adsorption of methylene blue and from the Randles-Shevchik equation (Table 6).

Table 4. Results of determining the specific capacity of the EDL of carbon felt

Sample	Specific capacity, F/g		
	Cyclic voltammetry	Charge-discharge curves	Electrochemical impedance spectroscopy (EIS)
1	0.21 ± 0.02	0.26 ± 0.05	0.28 ± 0.02
2	0.35 ± 0.02	0.42 ± 0.04	0.37 ± 0.02

Table 5. Results of determining the rate constant of heterogeneous electron transfer by various methods

Method	Sample No. 1	Sample No. 2	References
$k_s \cdot 10^3, \text{sm} \cdot \text{s}^{-1}, \text{CV}$	3 ± 1	3.1 ± 0.9	7.0 ± 0.5 [1]; 7 ± 3 [3]; 10 [5]
$k_s \cdot 10^3, \text{sm} \cdot \text{s}^{-1}, \text{EIS}$	3 ± 2	3 ± 2	3 ± 2 [5]; 7.7 ± 0.1 [42]

Table 6. Results of determining the content of the boundary plane by various methods

Sample	$k_s, \%$	$C_{\text{EDL}}, \%$	Ratio of specific areas, %
1	3 ± 1	2.7 ± 0.6	1.6 ± 0.4
2	3.1 ± 0.9	6.4 ± 0.9	4.4 ± 0.9

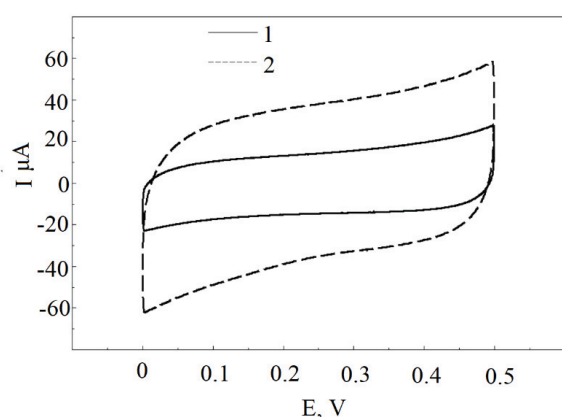


Fig. 4. Cyclic voltammograms of carbon felt in 0.1 M KCl; 1 – Sample No. 1, 2 – Sample No. 2

When calculating the capacity of the EDL, the specific capacity of the edge plane was taken as $70 \mu\text{F}\cdot\text{cm}^{-2}$, since in this case the result obtained is in good agreement with other methods. From the rectangular shape of the cyclic voltammograms of carbon felts (Fig. 4), one can conclude that there is no pseudocapacitance [41], therefore $70 \mu\text{F}\cdot\text{cm}^{-2}$ is the capacity of the EDL in the absence of pseudocapacitance. The distortion of the rectangular shape can be associated with the diffusion of ions to the electrode surface, which limits the charging rate [30].

Calculation from the values of the rate constant of heterogeneous electron transfer does not yield significant differences between the percentage content of the edge plane for the felts. This can be explained by the high error in determining this constant for this material [3, 43]. Calculations by other methods indicate a higher content of the edge plane in sample No. 2 despite the close values of the defect densities according to Raman spectroscopy data. Thus, the rate of electron transfer to the amorphous phase of carbon is low, which may be due to its low electrical conductivity. Charge accumulation also apparently occurs better on more structured graphite defects, which is associated with the formation of conjugated bond systems between quinoid structures.

4. Conclusion

It is shown that in order to obtain the most complete information on the surface area of a carbon material, it is necessary to use several complementary methods for its determination. Calculation of this value from cyclic voltammetry data with the help of the Randles-Shevchik equation, using potassium hexacyanoferrate (III) as an electrochemical sensor, makes it possible to determine predominantly the area

of the edge plane. Geometrical assessment of the surface area and determination by low-temperature gas adsorption should be used with caution. In the case of characterization of electrode materials, the expediency of using these methods is questionable. Comparing the specific surface area obtained by various methods with the results of Raman spectroscopy, it should be noted that electron transfer to amorphized carbon is more difficult than to crystalline carbon, while adsorption of methylene blue, on the contrary, occurs more easily on the amorphous phase.

5. Funding

The work was carried out with the financial support of the Ministry of Science and Higher Education of the Russian Federation within the framework of the state assignment No. FEWG-2024-0003 (Biocatalytic platforms based on microorganism cells, subcellular structures and enzymes in combination with nanomaterials).

6. Acknowledgements

We thank the staff of the Center for Collective Use of Scientific Equipment “Production and Application of Multifunctional Nanomaterials” of Tambov State Technical University for assistance in recording the Raman spectra of the studied samples.

7. Conflict of interests

The authors declare no conflict of interest.

References

1. Smith REG, Davies TJ, Baynes NDB, Nichols RJ. The electrochemical characterisation of graphite felts. *Journal of Electroanalytical Chemistry*. 2015;747:29-38. DOI:10.1016/j.jelechem.2015.03.029
2. Kroner I, Becker M, Turek T. Determination of rate constants and reaction orders of vanadium-ion kinetics on carbon fiber electrodes. *ChemElectroChem*. 2020;7:4314-4325. DOI:10.1002/celec.202001033
3. Landon-Lane L, Downard AJ, Marshall AT. Single fibre electrode measurements – A versatile strategy for assessing the non-uniform kinetics at carbon felt electrodes. *Electrochim Acta*. 2020;136709. DOI:10.1016/j.electacta.2020.136709
4. Wang K, Cao Z, Chang J, Sheng Y, et al. Promoted bioelectrocatalytic activity of microbial electrolysis cell (MEC) in sulfate removal through the synergy between neutral red and graphite felt. *Chemical Engineering Journal*. 2017;327:183-192. DOI:10.1016/j.cej.2017.06.086
5. Feynerol V, El Hage R, Brites Helú M, Fierro V, et al. Comparative kinetic analysis of redox flow battery electrolytes: From micro-fibers to macro-felts.

Electrochimica Acta. 2022;421:140373. DOI:10.1016/j.electacta.2022.140373

6. Maltsev AA, Bibikov SB, Varfolomeev SD, Kalinichenko VN, et al. Determining the specific surface area of carbon electrode materials for electrodes of supercapacitors via the adsorption of methylene blue dye. *Russian Journal of Physical Chemistry A*. 2018;92(4):772-777. DOI:10.1134/S0036024418040209

7. Kuzmina EV, Dmitrieva LR, Karaseva EV, Kolosnitsyn VS. On the possibility of application of the method of sorption of dyes for determining the specific surface area of carbon materials for lithium-sulfur batteries. *Izvestia Ufimskogo nauchnogo tsentra RAN*. 2020;2:29-34. DOI:10.31040/2222-8349-2020-0-2-29-34 (In Russ.)

8. Wen M, Liu H, Zhang F, Zhu Y, et al. Amorphous FeNiPt nanoparticles with tunable length for electrocatalysis and electrochemical determination of thiols. *Chemical Communications*. 2009;30:4530-4532. DOI:10.1039/B907379E

9. Zhu P, Zhao Y. Cyclic voltammetry measurements of electroactive surface area of porous nickel: Peak current and peak charge methods and diffusion layer effect. *Materials Chemistry and Physics*. 2019;233:60-67. DOI:10.1016/j.matchemphys.2019.05.034

10. Zou Y, Walton AS, Kinloch IA, Dryfe RAW. Investigation of the differential capacitance of highly ordered pyrolytic graphite as a model material of graphene. *Langmuir*. 2016;32(44):11448-11455. DOI:10.1021/acs.langmuir.6b02910

11. Rice RJ, McCreery RL. Quantitative relationship between electron transfer rate and surface microstructure of laser-modified graphite electrodes. *Analytical Chemistry*. 1989;61(15):1637-1641. DOI:10.1021/ac00190a010

12. Rice RJ, Pontikos NM, McCreery RL. Quantitative correlations of heterogeneous electron-transfer kinetics with surface properties of glassy carbon electrodes. *Journal of the American Chemical Society*. 1990;112(12):4617-4622. DOI:10.1021/ja00168a001

13. Iamprasertkun P, Hirunpinyopas W, Keerthi A, Wang B, et al. Capacitance of basal plane and edge-oriented highly ordered pyrolytic graphite: specific ion effects. *Journal of Physical Chemistry Letters*. 2019;10(3):617-623. DOI:10.1021/acs.jpcllett.8b03523

14. Yuan W, Zhou Y, Li Y, Li C, et al. The edge- and basal-plane-specific electrochemistry of a single-layer graphene sheet. *Scientific Reports*. 2013;3:2248. DOI:10.1038/srep02248

15. Pandolfo AG, Hollenkamp AF. Carbon properties and their role in supercapacitors. *Journal Power Sources*. 2006;157:11-27. DOI:10.1016/j.jpowsour.2006.02.065

16. McDermott MT, Kneten K, McCreery RL. Anthraquinonedisulfonate adsorption, electron-transfer kinetics, and capacitance on ordered graphite electrodes: the important role of surface defects. *Journal of Physical Chemistry*. 1992;96(7):3124-3130. DOI:10.1021/j100186a063

17. Velický M, Toth PS, Woods CR, Novoselov KS, Dryfe RAW. Electrochemistry of the basal plane versus edge plane of graphite revisited. *Journal of Physical*

Chemistry C. 2019;123(18):11677-11685. DOI:10.1021/acs.jpcc.9b01010

18. Li Y, Li Q, Wang H, Zhang L, et al. Recent progresses in oxygen reduction reaction electrocatalysts for electrochemical energy applications. *Electrochemical Energy Reviews*. 2019;2:518-538. DOI:10.1007/s41918-019-00052-4

19. Ramesh P, Sampath S. Electrochemical characterization of binderless, recompressed exfoliated graphite electrodes: electron-transfer kinetics and diffusion characteristics. *Analytical Chemistry*. 2003;75(24):6949-6957. DOI:10.1021/ac034833u

20. Chen P, McCreery RL. Control of electron transfer kinetics at glassy carbon electrodes by specific surface modification. *Analytical Chemistry*. 1996;68(22):3958-3965. DOI:10.1021/ac960492r

21. Kneten KR, McCreery RL. Effects of redox system structure on electron-transfer kinetics at ordered graphite and glassy carbon electrodes. *Analytical Chemistry*. 1992;64(21):2518-2524. DOI:10.1021/ac00045a011

22. McCreery RL, McDermott MT. Comment on electrochemical kinetics at ordered graphite electrodes. *Analytical Chemistry*. 2012;84:2602-2605. DOI:10.1021/ac2031578

23. Abdelrahim AM, Abd El-Moghny MG, El-Shakre ME, El-Deab MS. High mass loading MnO₂/graphite felt electrode with marked stability over a wide potential window of 1.9 V for supercapacitor application. *Journal of Energy Storage*. 2023;57:106218. DOI:10.1016/j.est.2022.106218

24. Rosolen JM, Matsubara EY, Marchesin MS, Lala SM, et al. Carbon nanotube/felt composite electrodes without polymer binders. *Journal Power Sources*. 2006;162(1):620-628. DOI:10.1016/j.jpowsour.2006.06.087

25. Emmel D, Hofmann JD, Arlt T, Manke I, et al. Understanding the impact of compression on the active area of carbon felt electrodes for redox flow batteries. *ACS Applied Energy Materials*. 2020;3(5):4384-4393. DOI:10.1021/acs.aem.0c00075

26. Das I, Das S, Ghangrekar MM. Application of bimetallic low-cost CuZn as oxygen reduction cathode catalyst in lab-scale and field-scale microbial fuel cell. *Chemical Physics Letters*. 2020;751:137536. DOI:10.1016/j.cplett.2020.137536

27. Randviir EP. A cross examination of electron transfer rate constants for carbon screen-printed electrodes using Electrochemical Impedance Spectroscopy and cyclic voltammetry. *Electrochimica Acta*. 2018;286:179-186. DOI:10.1016/j.electacta.2018.08.021

28. Lavagnini I, Antiochia R, Magno F. An extended method for the practical evaluation of the standard rate constant from cyclic voltammetric data. *Electroanalysis*. 2004;16(6):505-506. DOI:10.1002/elan.200302851

29. Lazanas AC, Prodromidis MI. Electrochemical impedance spectroscopy – A Tutorial. *ACS Measurement Science Au*. 2022;3:162-193. DOI:10.1021/acsmeasuresciau.2c00070

30. Wei L, Sevilla M, Fuertes AB, Mokaya R, Yushin G. Hydrothermal carbonization of abundant renewable natural organic chemicals for high-performance supercapacitor electrodes. *Advanced Energy Materials*. 2011;1(3):356-361. DOI:10.1002/aenm.201100019
31. Li Z, Deng L, Kinloch IA, Young RJ. Raman spectroscopy of carbon materials and their composites: Graphene, nanotubes and fibres. *Progress in Materials Science*. 2023;135. DOI:10.1016/j.pmatsci.2023.101089
32. Chernyak SA, Ivanov AS, Stolbov DN, Egorova TB, et al. N-doping and oxidation of carbon nanotubes and jellyfish-like graphene nanoflakes through the prism of Raman spectroscopy. *Applied Surface Science*. 2019;488:51-60. DOI:10.1016/j.apsusc.2019.05.243
33. Ghosh S, Ganesan K, Polaki SR, Ravindran TR, et al. Evolution and defect analysis of vertical graphene nanosheets. *Journal of Raman Spectroscopy*. 2014;45(8):642-649. DOI:10.1002/jrs.4530
34. Bonpua J, Yagües Y, Aleshin A, Dasappa S, Camacho J. Flame temperature effect on sp² bonds on nascent carbon nanoparticles formed in premixed flames (T_{f,max} > 2100 K): A Raman spectroscopy and particle mobility sizing study. *Proceedings of the Combustion Institute*. 2019;37(1):943-951. DOI:10.1016/j.proci.2018.06.124
35. Cançado LG, Jorio A, Ferreira EHM, Stavale F, et al. Quantifying defects in graphene via Raman spectroscopy at different excitation energies. *Nano Letters*. 2011;11(8):3190-3196. DOI:10.1021/nl201432g
36. Ribeiro-Soares J, Oliveros ME, Garin C, David MV, et al. Structural analysis of polycrystalline graphene systems by Raman spectroscopy. *Carbon*. 2015;95:646-652. DOI:10.1016/j.carbon.2015.08.020
37. Eckmann A, Felten A, Mishchenko A, Britnell L, et al. Probing the nature of defects in graphene by Raman spectroscopy. *Nano Letters*. 2012;12:3925-3930. DOI:10.1021/nl300901a
38. Venezuela P, Lazzeri M, Mauri F. Theory of double-resonant Raman spectra in graphene: Intensity and line shape of defect-induced and two-phonon bands. *Physical Review B – Condensed Matter and Materials Physics*. 2011;84:035433. DOI:10.1103/PhysRevB.84.035433
39. Ferrari AC, Basko DM. Raman spectroscopy as a versatile tool for studying the properties of graphene. *Nature Nanotechnology*. 2013;8:235-246. DOI:10.1038/nnano.2013.46
40. Huang Le TX, Bechelany M, Cretin M. Carbon felt based-electrodes for energy and environmental applications: A review. *Carbon*. 2017;122:564-591. DOI:10.1016/j.carbon.2017.06.078
41. Morales DM, Risch M. Seven steps to reliable cyclic voltammetry measurements for the determination of double layer capacitance. *JPhys Energy*. 2021;3(3):034013. DOI:10.1088/2515-7655/abee33
42. Landon-Lane L, Marshall AT, Harrington DA. EIS at carbon fiber cylindrical microelectrodes. *Electrochemistry Communications*. 2019;109:106566. DOI:10.1016/j.elecom.2019.106566
43. Rabbow TJ, Trampert M, Pokorny P, Binder P, Whitehead AH. Variability within a single type of polyacrylonitrile-based graphite felt after thermal treatment. Part II: Chemical properties. *Electrochimica Acta*. 2015;173:24-30. DOI:10.1016/j.electacta.2015.05.058

Information about the authors / Информация об авторах

Pavel V. Oskin, Junior Researcher, Tula State University (TulSU), Tula, Russian Federation; ORCID 0000-0001-9308-6496; e-mail: pavelfraj@yandex.ru

Roman V. Lepikash, Junior Researcher, TulSU, Tula, Russian Federation; ORCID 0000-0001-7853-2937; e-mail: mr.romalep@yandex.ru

Tatyana P. Dyachkova, D. Sc. (Chem.), Professor, Tambov State Technical University, Tambov, Russian Federation; ORCID 0000-0002-4884-5171; e-mail: dyachkova_tp@mail.ru

Sergey V. Alferov, Cand. Sc. (Chem.), Associate Professor, Head of the Laboratory, TulSU, Tula, Russian Federation; ORCID 0000-0002-5217-7815; e-mail: s.v.alferov@gmail.com

Оськин Павел Владимирович, младший научный сотрудник, Тульский государственный университет (ТулГУ), Тула, Российская Федерация; ORCID 0000-0001-9308-6496; e-mail: pavelfraj@yandex.ru

Лепикаш Роман Владимирович, младший научный сотрудник, ТулГУ, Тула, Российская Федерация; ORCID 0000-0001-7853-2937; e-mail: mr.romalep@yandex.ru

Дьячкова Татьяна Петровна, доктор химических наук, профессор, Тамбовский государственный технический университет, Тамбов, Российская Федерация; ORCID 0000-0002-4884-5171; e-mail: dyachkova_tp@mail.ru

Алферов Сергей Валерьевич, кандидат химических наук, доцент, заведующий лабораторией, ТулГУ, Тула, Российская Федерация; ORCID 0000-0002-5217-7815; e-mail: s.v.alferov@gmail.com

Received 13 May 2024; Accepted 14 August 2024; Published 22 October 2024



Copyright: © Oskin PV, Lepikash RV, Dyachkova TP, Alferov SV, 2024. This article is an open access article distributed under the terms and conditions of the Creative Commons Attribution (CC BY) license (<https://creativecommons.org/licenses/by/4.0/>).